PWNCAT2

Lots of people...

ABSTRACT

Abstract goes here

Subject headings: Catalogs; Fermi Gamma-ray Space Telescope; Gamma rays: observations; pulsar wind nebula

*Todo list

1. Introduction

The introduction goes here...

Primary motivations for improved analysis

- More data (3 years vs 18 months)

- Many new GeV pulsars
- Hope to find new PWN in the off-peak emission of LAT-detected GeV Pulsars.
- Going to higher energies thanks to improved IRFs.
- Better spatial/morphological analysis due to new `pointlike` code.

2. LAT Description and Observations

Description goes here...

We used the same data set as that used in the second *Fermi*-LAT pulsar catalog. In particular, this data set spans 3 years from XXXXXXto XXXXXX.

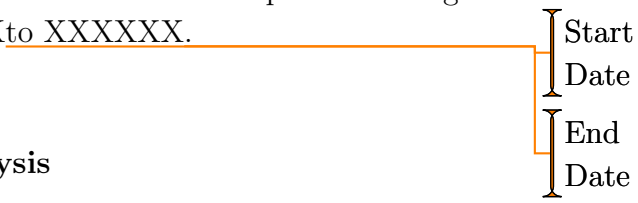

3. Timing Analysis

Timing analysis goes here...

4. Off-peak Phase Selection

To study the off-peak emission of LAT-detected pulsars, we first developed a new method for defining the off-peak emission. The primary constraint for this method was that it was systematic, computationally efficient and model independent, and that it correctly removed the pulsed emission for already studied pulsars.

The method we developed is

- First, deconstruct the pulsar phaseogram using a Bayseian blocks representation of the data.
  - Figure 1 shows the off peak selection for some pulsars...
  - Set the ncpPrior parameter to 5
- Before beinning the data, first rotate the maximum phase range to 0 so that the off-peak region will not overlap the phase edge.
-

required first representing the

THe off peak phase range is defined in Table 1.

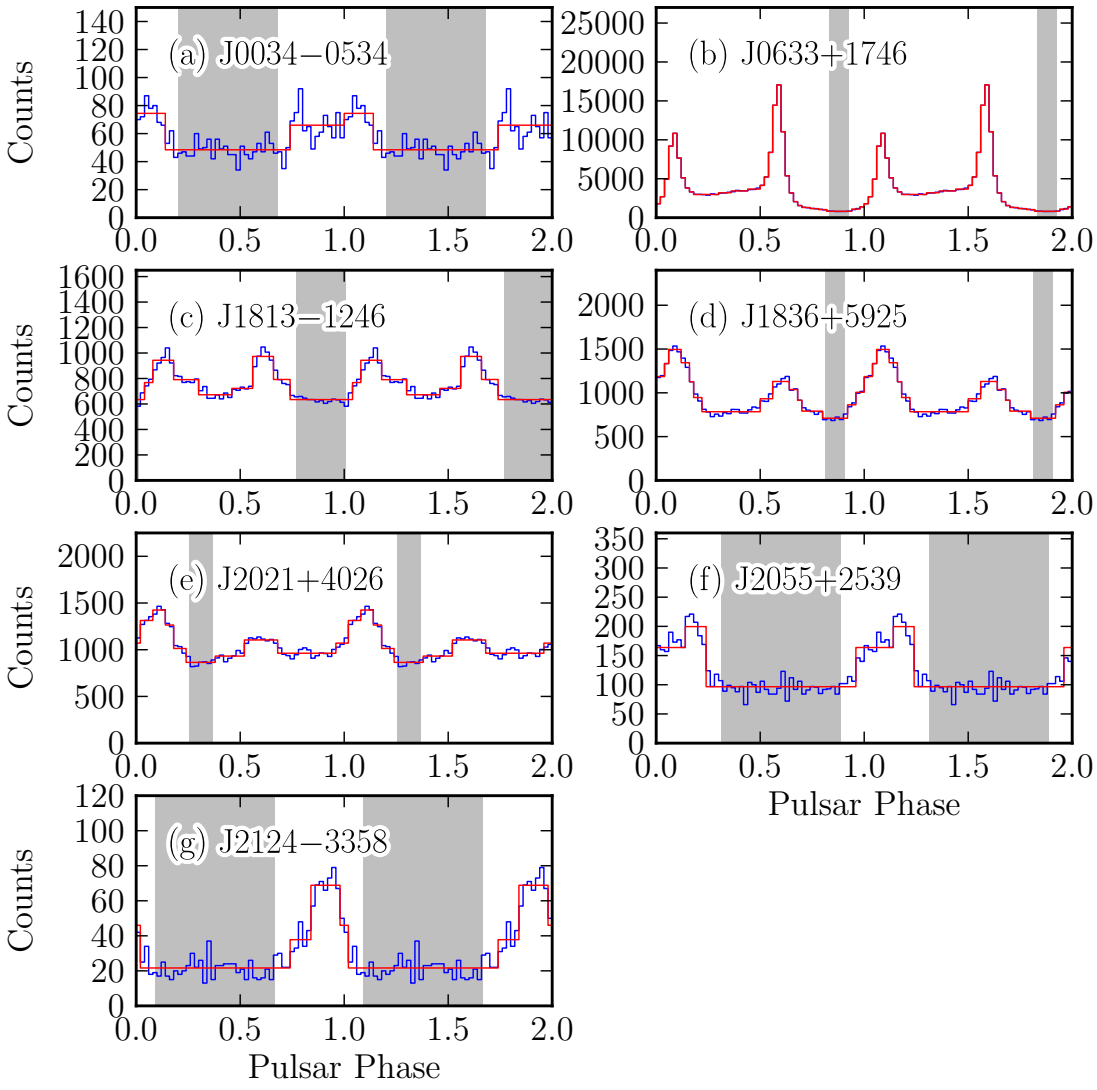

Fig. 1.— Off peak selection for some pulsars...

Table 1. Timing Observatories, definition of the off-peak region, and pulsar distances.

PSR	ObsID	Phase	Distance	Observation period rejected (MJD)
J0007+7303	···	0.53 - 0.91	···	···
J0030+0451	···	0.71 - 0.05	···	···
J0034−0534	···	0.21 - 0.68	···	···
J0106+4855	···	0.24 - 0.54	···	···
J0218+4232	···	0.83 - 0.17	···	···
J0248+6021	···	0.56 - 0.12	···	···
J0340+4130	···	0.17 - 0.64	···	···
J0357+3205	···	0.37 - 0.85	···	···
J0437−4715	···	0.60 - 0.16	···	···
J0534+2200	···	0.60 - 0.84	···	···
J0610−2100	···	0.29 - 0.51	···	···
J0613−0200	···	0.57 - 0.05	···	···
J0614−3329	···	0.36 - 0.50	···	···
J0622+3749	···	0.31 - 0.87	···	···
J0631+1036	···	0.64 - 0.19	···	···
J0633+0632	···	0.65 - 0.96	···	···
J0633+1746	···	0.84 - 0.92	···	···
J0659+1414	···	0.41 - 0.04	···	···
J0729−1448	···	0.70 - 0.42	···	···
J0734−1559	···	0.33 - 0.83	···	···
J0742−2822	···	0.73 - 0.37	···	···
J0751+1807	···	0.75 - 0.29	···	···
J0835−4510	···	0.85 - 0.03	···	···
J0908−4913	···	0.17 - 0.53	···	···
J0940−5428	···	0.56 - 0.14	···	···
J1016−5857	···	0.62 - 0.01	···	···
J1019−5749	···	0.66 - 0.37	···	···
J1023−5746	···	0.67 - 0.01	···	···
J1024−0719	···	0.88 - 0.34	···	···
J1028−5819	···	0.77 - 0.08	···	···
J1044−5737	···	0.56 - 0.96	···	···
J1048−5832	···	0.67 - 0.03	···	···
J1057−5226	···	0.16 - 0.56	···	···
J1105−6107	···	0.69 - 0.03	···	···
J1119−6127	···	0.60 - 0.18	···	···
J1135−6055	···	0.44 - 0.86	···	···
J1231−1411	···	0.86 - 0.10	···	···
J1357−6429	···	0.79 - 0.01	···	···
J1410−6132	···	0.51 - 0.89	···	···
J1413−6205	···	0.58 - 0.02	···	···
J1418−6058	···	0.66 - 0.92	···	···
J1420−6048	···	0.57 - 0.05	···	···
J1429−5911	···	0.32 - 0.42	···	···
J1459−6053	···	0.33 - 0.67	···	···
J1509−5850	···	0.65 - 0.13	···	···

Table 1—Continued

PSR	ObsID	Phase	Distance	Observation period rejected (MJD)
J1513−5908	···	0.52 - 0.12	···	···
J1531−5610	···	0.55 - 0.19	···	···
J1600−3053	···	0.53 - 0.09	···	···
J1614−2230	···	0.83 - 0.17	···	···
J1620−4927	···	0.54 - 0.98	···	···
J1702−4128	···	0.58 - 0.16	···	···
J1709−4429	···	0.75 - 0.07	···	···
J1713+0747	···	0.67 - 0.19	···	···
J1718−3825	···	0.01 - 0.19	···	···
J1732−3131	···	0.79 - 0.95	···	···
J1741−2054	···	0.47 - 0.97	···	···
J1744−1134	···	0.16 - 0.72	···	···
J1746−3239	···	0.42 - 0.98	···	···
J1747−2958	···	0.66 - 0.10	···	···
J1803−2149	···	0.58 - 0.02	···	···
J1809−2332	···	0.53 - 0.91	···	···
J1813−1246	···	0.78 - 0.01	···	···
J1823−3021A	···	0.09 - 0.56	···	···
J1826−1256	···	0.26 - 0.52	···	···
J1836+5925	···	0.82 - 0.90	···	···
J1846+0919	···	0.42 - 0.88	···	···
J1907+0602	···	0.69 - 0.05	···	···
J1939+2134	···	0.09 - 0.47	···	···
J1952+3252	···	0.73 - 0.05	···	···
J1954+2836	···	0.67 - 0.98	···	···
J1957+5033	···	0.44 - 0.90	···	···
J1958+2846	···	0.64 - 0.92	···	···
J1959+2048	···	0.79 - 0.97	···	···
J2017+0603	···	0.76 - 0.20	···	···
J2021+3651	···	0.74 - 0.98	···	···
J2021+4026	···	0.26 - 0.36	···	···
J2028+3332	···	0.58 - 0.97	···	···
J2030+3641	···	0.71 - 0.21	···	···
J2030+4415	···	0.94 - 0.02	···	···
J2032+4127	···	0.68 - 0.92	···	···
J2043+2740	···	0.64 - 0.04	···	···
J2051−0827	···	0.77 - 0.24	···	···
J2055+2539	···	0.39 - 0.86	···	···
J2124−3358	···	0.14 - 0.58	···	···
J2139+4716	···	0.27 - 0.90	···	···
J2214+3000	···	0.64 - 0.74	···	···
J2238+5903	···	0.65 - 0.99	···	···
J2240+5832	···	0.70 - 0.46	···	···
J2302+4442	···	0.75 - 0.23	···	···

Note. —

Put table comments

5. Analysis of the *Fermi*-LAT data

Methods for data analysis

- Cut on pulsar phase
- Perform localization or extension fitting using `gtlike` using energies from 1 GeV to 316 GeV.
- If it is point-like, perform an extension upper limit analysis
- Perform spectral analysis using `gtlike` for energies above 100 MeV to 316 GeV.
- There is a detection if TS $>$ 25 in the point-like source hypothesis after fitting the position of the point-like source.
- Consider the source to be extended if $TS_{ext} > 16$. Similar to extended source search paper .
- Calculate TS_{cutoff} for all energies.

cite extended source search paper

5.1. Variability

5.2. When to consider the source a pulsar or PWN.

- If extended, then it is a PWN (cannot be a pulsar)
- If it is significiant for $E > 10$ GeV, it is a PWN (too hard to be a pulsar)
- Otherwise, if it has a cutoff, it is a Pulsar candidate
- For point-like emission that is not significantly cutoff, the emission mechanism is uncertain.

6. Results

First, we tested the sources to see if they were spatially extended. The localization results are in Table 2.

Next, we performed a spectral analysis over all energy using the best fit morphology. Table 3 shows the results of the all energy analysis of the off-peak emission for each pulsar.

Table 2. Localization and extension fitting results

PSR	TS_{point}	GLON (deg)	GLAT (deg)	Pos Err	Offset (deg)	TS_{ext}	Extension (deg)
J0007+7303	84.0	119.64	10.35	0.11	0.11	9.5	< 0.40
J0034−0534	42.4	111.53	-68.03	0.06	0.04	0.0	< 0.12
J0218+4232	34.7	139.56	-17.53	0.08	0.05	0.0	< 0.15
J0340+4130	25.1	153.81	-11.00	0.06	0.04	0.0	< 0.13
J0534+2200	4959.1	184.55	-5.79	0.01	0.01	0.0	< 0.02
J0633+1746	2842.4	195.12	4.22	0.02	0.05	3.3	< 0.09
J0835−4510	304.7	263.46	-3.15	0.08	0.37	295.3	0.73 ± 0.06
J1023−5746	83.0	285.52	-0.08	0.14	1.39	190.4	1.40 ± 0.10
J1119−6127	123.2	291.97	-0.61	0.06	0.20	41.0	0.29 ± 0.06
J1513−5908	122.6	320.34	-1.20	0.02	0.04	0.0	< 0.12
J1620−4927	39.1	333.87	0.25	0.05	0.16	0.0	< 0.34
J1709−4429	30.7	342.50	-3.70	0.52	1.18	29.2	1.18 ± 0.24
J1744−1134	74.4	14.79	9.18	None	0.00	0.0	< 2.83
J1746−3239	47.6	357.60	-1.30	None	1.08	139.2	2.07 ± 0.14
J1747−2958	30.3	358.66	0.29	0.14	1.31	43.8	1.94 ± 0.13
J1809−2332	29.0	7.33	-2.26	0.14	0.27	14.6	< 0.39
J1813−1246	53.3	17.32	2.46	0.05	0.07	0.2	< 0.25
J1836+5925	5019.4	88.87	25.00	0.01	0.00	0.0	< 0.06
J2021+4026	920.6	78.24	2.10	0.02	0.02	16.1	0.11 ± 0.03
J2032+4127	28.5	79.78	0.78	None	0.50	62.8	1.25 ± 0.18
J2055+2539	109.0	70.68	-12.45	0.06	0.07	0.0	< 0.14
J2124−3358	106.5	10.83	-45.40	0.04	0.07	0.0	< 0.09
J2302+4442	115.0	103.36	-14.04	0.05	0.05	0.9	< 0.22

Note. —

Put table comments

Next, we fit a powerlaw independently in each energy bin. Table 4 shows the results of the analysis in separate energy bins of each pulsar.

Finally, we tested sources to see which were variable. Table 5 shows the results of the cutoff test for pulsars with significant low-energy emission.

Table 3. All Energy spectral fit for the

How many pulsars?

LAT-detected Pulsars

PSR	TS	$F_{0.1-316}$ (10^{-9} ph cm^{-2} s^{-1})	$G_{0.1-316}$ (10^{-12} erg cm^{-2}s^{-1})	Γ	Luminosity (10^{33} erg s^{-1})
J0007+7303	84.0	53.36 ± 9.81	20.08 ± 2.37	2.74 ± 0.19	None
J0030+0451	14.1	< 8.22	< 10.61	···	None
J0034−0534	42.4	16.05 ± 4.75	8.52 ± 1.65	2.41 ± 0.19	None
J0106+4855	0.0	< 6.80	< 8.78	···	None
J0218+4232	34.7	50.61 ± 20.56	18.40 ± 3.35	2.78 ± 0.48	None
J0248+6021	18.8	< 13.60	< 17.56	···	None
J0340+4130	25.1	10.28 ± 3.62	9.32 ± 2.46	2.13 ± 0.15	None
J0357+3205	0.0	< 2.97	< 3.83	···	None
J0437−4715	0.0	< 1.85	< 2.39	···	None
J0534+2200	4959.1	559.71 ± 19.47	397.02 ± 12.21	2.24 ± 0.02	None
J0610−2100	0.0	< 3.23	< 4.17	···	None
J0613−0200	0.0	< 3.37	< 4.35	···	None
J0614−3329	15.6	< 15.81	< 20.41	···	None
J0622+3749	1.0	< 7.81	< 10.08	···	None
J0631+1036	14.5	< 13.79	< 17.80	···	None
J0633+0632	4.1	< 10.19	< 13.16	···	None
J0633+1746	2842.4	882.74 ± 30.65	579.06 ± 23.61	2.28 ± 0.03	None
J0659+1414	0.0	< 1.77	< 2.29	···	None
J0729−1448	0.0	< 4.85	< 6.25	···	None
J0734−1559	24.5	< 12.39	< 16.00	···	None
J0742−2822	4.3	< 6.84	< 8.83	···	None
J0751+1807	8.1	< 5.70	< 7.36	···	None
J0835−4510	600.0	389.91 ± 22.62	327.74 ± 20.41	2.16 ± 0.03	None
J0908−4913	15.1	< 24.71	< 31.89	···	None
J0940−5428	0.0	< 1.73	< 2.24	···	None
J1016−5857	0.0	< 12.09	< 15.61	···	None
J1019−5749	2.4	< 12.59	< 16.25	···	None
J1023−5746	273.4	399.13 ± 37.06	472.93 ± 35.48	2.03 ± 0.04	None
J1024−0719	0.0	< 2.30	< 2.97	···	None
J1028−5819	8.0	< 26.93	< 34.77	···	None
J1044−5737	0.0	< 17.76	< 22.92	···	None
J1048−5832	0.0	< 16.77	< 21.65	···	None
J1057−5226	0.8	< 5.03	< 6.49	···	None
J1105−6107	11.0	< 31.71	< 40.93	···	None
J1119−6127	164.2	112.84 ± 3.58	92.50 ± 2.17	2.17 ± 0.01	None
J1135−6055	4.2	< 6.89	< 8.89	···	None
J1231−1411	0.0	< 3.21	< 4.14	···	None
J1357−6429	0.0	< 5.72	< 7.38	···	None
J1410−6132	18.4	< 42.29	< 54.59	···	None
J1413−6205	0.0	< 11.99	< 15.48	···	None
J1418−6058	0.0	< 34.10	< 44.02	···	None
J1420−6048	12.1	< 31.86	< 41.13	···	None
J1429−5911	0.0	< 12.66	< 16.34	···	None
J1459−6053	0.0	< 9.08	< 11.72	···	None
J1509−5850	0.0	< 9.66	< 12.47	···	None

Table 3—Continued

PSR	TS	$F_{0.1-316}$ (10^{-9} ph cm^{-2} s^{-1})	$G_{0.1-316}$ (10^{-12} erg cm^{-2}s^{-1})	Γ	Luminosity (10^{33} erg s^{-1})
J1513−5908	122.6	19.15 ± 7.39	51.40 ± 8.43	1.79 ± 0.12	None
J1531−5610	0.5	< 3.52	< 4.54	···	None
J1600−3053	0.0	< 1.85	< 2.39	···	None
J1614−2230	0.9	< 5.93	< 7.65	···	None
J1620−4927	39.1	79.65 ± 20.62	64.27 ± 11.41	2.18 ± 0.10	None
J1702−4128	0.0	< 5.75	< 7.42	···	None
J1709−4429	69.0	181.80 ± 36.37	90.11 ± 34.30	2.46 ± 0.41	None
J1713+0747	0.0	< 4.79	< 6.18	···	None
J1718−3825	0.0	< 14.54	< 18.78	···	None
J1732−3131	0.0	< 8.65	< 11.16	···	None
J1741−2054	0.0	< 13.38	< 17.27	···	None
J1744−1134	74.4	47.10 ± 8.73	27.61 ± 3.67	2.34 ± 0.08	None
J1746−3239	186.8	461.05 ± 37.05	624.30 ± 40.49	1.98 ± 0.03	None
J1747−2958	74.0	260.88 ± 40.86	512.22 ± 68.60	1.87 ± 0.04	None
J1803−2149	6.1	< 27.06	< 34.93	···	None
J1809−2332	29.0	85.89 ± 68.64	43.14 ± 9.05	2.45 ± 0.62	None
J1813−1246	53.3	191.30 ± 40.97	83.32 ± 11.83	2.57 ± 0.14	None
J1823−3021A	2.7	< 5.16	< 6.66	···	None
J1826−1256	18.4	< 66.21	< 85.47	···	None
J1836+5925	5019.4	561.39 ± 17.71	538.66 ± 25.37	2.11 ± 0.02	None
J1846+0919	0.0	< 3.35	< 4.32	···	None
J1907+0602	0.0	< 7.27	< 9.39	···	None
J1939+2134	0.0	< 4.40	< 5.68	···	None
J1952+3252	0.4	< 7.78	< 10.05	···	None
J1954+2836	6.1	< 18.52	< 23.91	···	None
J1957+5033	0.0	< 2.52	< 3.26	···	None
J1958+2846	0.0	< 7.72	< 9.97	···	None
J1959+2048	0.0	< 4.89	< 6.32	···	None
J2017+0603	0.0	< 2.97	< 3.83	···	None
J2021+3651	0.1	< 7.88	< 10.18	···	None
J2021+4026	936.6	1196.46 ± 26.76	824.96 ± 13.64	2.25 ± 0.01	None
J2028+3332	0.0	< 4.57	< 5.90	···	None
J2030+3641	0.0	< 2.89	< 3.73	···	None
J2030+4415	3.5	< 28.40	< 36.66	···	None
J2032+4127	91.3	192.51 ± 51.56	425.89 ± 53.73	1.84 ± 0.08	None
J2043+2740	0.0	< 2.58	< 3.33	···	None
J2051−0827	0.0	< 1.89	< 2.44	···	None
J2055+2539	109.0	46.79 ± 6.38	21.45 ± 2.28	2.52 ± 0.08	None
J2124−3358	106.5	20.21 ± 3.88	18.48 ± 3.09	2.13 ± 0.10	None
J2139+4716	16.8	< 9.29	< 11.99	···	None
J2214+3000	0.0	< 5.02	< 6.48	···	None
J2238+5903	0.0	< 6.19	< 7.99	···	None
J2240+5832	0.0	< 6.37	< 8.22	···	None
J2302+4442	115.0	33.65 ± 5.34	18.69 ± 2.23	2.38 ± 0.10	None

Note. —

Put table comments

Table 4. Energy bin spectral fit for the

How many pulsars?

LAT-detected Pulsars

PSR	$TS_{0.1-1}$	$F_{0.1-1}$ (10^{-9} ph cm^{-2} s^{-1})	$\Gamma_{0.1-1}$	TS_{1-10}	F_{1-10} (10^{-9} ph cm^{-2} s^{-1})	Γ_{1-10}	TS_{10-316}	F_{10-316} (10^{-9} ph cm^{-2} s^{-1})	Γ_{10-316}
J0007+7303	80.0	54.31 ± 9.26	2.79 ± -0.25	25.7	1.15 ± 0.28	2.80 ± -0.61	0.6	< 0.07	···
J0030+0451	16.9	< 1.84	···	4.5	< 0.14	···	0.0	< 0.15	···
J0034−0534	19.9	< 1.52	···	28.2	0.72 ± 0.52	2.90 ± -0.53	0.0	< 0.07	···
J0106+4855	23.2	< 1.62	···	2.6	< 0.16	···	0.0	< 0.08	···
J0218+4232	19.1	< 2.81	···	17.3	< 0.13	···	0.0	< 0.07	···
J0248+6021	25.4	39.60 ± 18.25	2.39 ± -0.40	6.1	< 0.11	···	2.2	< 0.05	···
J0340+4130	0.6	< 0.95	···	42.1	1.40 ± 0.37	2.93 ± -0.24	0.0	< 0.07	···
J0357+3205	0.0	< 0.55	···	0.0	< 0.08	···	0.0	< 0.09	···
J0437−4715	11.8	< 0.41	···	0.0	< 0.05	···	0.0	< 0.06	···
J0534+2200	3015.1	800.24 ± 23.70	3.17 ± -0.05	2115.7	27.73 ± 1.66	1.73 ± -0.08	1210.9	5.27 ± 1.51	2.17 ± -0.14
J0610−2100	0.0	< 0.56	···	0.0	< 0.24	···	0.0	< 0.13	···
J0613−0200	0.1	< 0.99	···	2.2	< 0.06	···	0.0	< 0.07	···
J0614−3329	16.1	< 2.74	···	9.4	< 0.20	···	0.0	< 0.22	···
J0622+3749	10.0	< 1.58	···	17.3	< 0.08	···	0.0	< 0.07	···
J0631+1036	12.3	< 2.67	···	5.1	< 0.17	···	2.6	< 0.06	···
J0633+0632	5.0	< 2.66	···	3.1	< 0.28	···	3.7	< 0.16	···
J0633+1746	2346.7	695.27 ± 31.74	1.82 ± -0.06	984.1	41.63 ± 2.64	3.42 ± -0.17	0.0	< 0.37	···
J0659+1414	0.0	< 0.37	···	0.2	< 0.09	···	0.0	< 0.05	···
J0729−1448	6.7	< 1.15	···	3.8	< 0.10	···	0.0	< 0.05	···
J0734−1559	38.1	41.17 ± 8.35	2.32 ± -0.24	3.8	< 0.10	···	0.0	< 0.07	···
J0742−2822	7.4	< 1.49	···	0.2	< 0.11	···	2.9	< 0.07	···
J0751+1807	1.5	< 0.71	···	10.4	< 0.18	···	0.0	< 0.06	···
J0835−4510	470.4	329.73 ± 26.66	1.98 ± -0.10	274.9	28.20 ± 2.13	2.32 ± -0.13	15.6	< 0.44	···
J0908−4913	22.8	< 5.57	···	5.3	< 0.15	···	0.0	< 0.07	···
J0940−5428	0.0	< 0.47	···	0.0	< 0.06	···	0.0	< 0.04	···
J1016−5857	0.0	< 2.67	···	0.4	< 0.22	···	0.0	< 0.07	···
J1019−5749	113.3	54.35 ± 14.54	1.22 ± -0.30	11.8	< 0.34	···	0.0	< 0.05	···
J1023−5746	383.6	359.20 ± 48.52	1.94 ± -0.15	213.0	39.00 ± 5.53	2.21 ± -0.14	68.4	3.00 ± 0.53	1.94 ± -0.18
J1024−0719	0.9	< 0.38	···	0.1	< 0.11	···	0.0	< 0.07	···
J1028−5819	0.7	< 3.40	···	8.1	< 0.25	···	0.0	< 0.11	···
J1044−5737	50.8	74.83 ± 6.91	2.31 ± -0.11	12.5	< 0.16	···	0.0	< 0.08	···
J1048−5832	6.3	< 4.25	···	9.2	< 0.37	···	0.0	< 0.09	···
J1057−5226	0.7	< 1.04	···	3.0	< 0.17	···	0.0	< 0.06	···
J1105−6107	0.0	< 2.27	···	20.2	< 0.24	···	0.0	< 0.12	···

Table 4—Continued

PSR	$TS_{0.1-1}$	$F_{0.1-1}$ (10^{-9} ph cm^{-2} s^{-1})	$\Gamma_{0.1-1}$	TS_{1-10}	F_{1-10} (10^{-9} ph cm^{-2} s^{-1})	Γ_{1-10}	TS_{10-316}	F_{10-316} (10^{-9} ph cm^{-2} s^{-1})	Γ_{10-316}
J1119−6127	108.2	58.52 ± 12.12	1.42 ± -0.26	22.1	< 0.80	···	12.0	< 0.11	···
J1135−6055	4.5	< 2.60	···	0.0	< 0.09	···	3.8	< 0.09	···
J1231−1411	0.8	< 0.86	···	0.0	< 0.15	···	0.0	< 0.13	···
J1357−6429	0.0	< 1.01	···	0.0	< 0.26	···	2.8	< 0.17	···
J1410−6132	0.1	< 3.58	···	14.3	< 0.58	···	5.1	< 0.08	···
J1413−6205	0.0	< 1.36	···	3.9	< 0.43	···	0.0	< 0.06	···
J1418−6058	0.0	< 2.70	···	11.3	< 0.73	···	1.6	< 0.13	···
J1420−6048	3.2	< 5.61	···	5.6	< 0.46	···	7.8	< 0.08	···
J1429−5911	0.0	< 2.55	···	0.0	< 0.41	···	1.2	< 0.26	···
J1459−6053	3.7	< 3.33	···	0.5	< 0.21	···	0.0	< 0.08	···
J1509−5850	0.0	< 1.82	···	0.5	< 0.25	···	0.1	< 0.05	···
J1513−5908	25.5	59.03 ± 22.17	2.51 ± -0.34	39.7	2.77 ± 0.70	2.14 ± -0.33	73.8	0.51 ± 0.01	1.79 ± -0.02
J1531−5610	0.0	< 1.41	···	0.0	< 0.11	···	0.2	< 0.05	···
J1600−3053	0.0	< 0.46	···	0.0	< 0.08	···	0.0	< 0.05	···
J1614−2230	0.5	< 0.89	···	4.7	< 0.14	···	0.0	< 0.09	···
J1620−4927	51.7	61.44 ± 9.48	1.20 ± -0.19	82.5	10.49 ± 1.51	3.50 ± -0.42	12.7	< 0.16	···
J1702−4128	0.0	< 1.80	···	0.0	< 0.13	···	0.0	< 0.06	···
J1709−4429	79.4	168.69 ± 22.93	2.39 ± -0.16	17.5	< 1.38	···	0.0	< 0.14	···
J1713+0747	5.1	< 1.22	···	0.8	< 0.09	···	0.0	< 0.06	···
J1718−3825	0.0	< 2.80	···	0.0	< 0.41	···	0.0	< 0.16	···
J1732−3131	0.0	< 2.87	···	0.0	< 0.31	···	0.0	< 0.19	···
J1741−2054	3.0	< 2.00	···	4.8	< 0.12	···	7.7	< 0.06	···
J1744−1134	28.7	31.48 ± 10.37	1.99 ± -0.33	58.5	2.80 ± 0.45	2.95 ± -0.39	0.4	< 0.06	···
J1746−3239	103.4	226.48 ± 59.36	1.74 ± -0.21	281.9	62.83 ± 4.92	2.21 ± -0.14	27.3	3.15 ± 0.18	2.14 ± -0.04
J1747−2958	0.0	< 7.41	···	327.7	86.20 ± 9.14	2.09 ± -0.11	4.3	< 0.21	···
J1803−2149	0.4	< 3.51	···	4.4	< 0.50	···	1.2	< 0.10	···
J1809−2332	42.4	46.80 ± 84.36	1.38 ± -1.68	19.5	< 0.34	···	2.0	< 0.12	···
J1813−1246	50.6	148.54 ± 30.26	2.36 ± -0.26	32.1	5.61 ± 4.19	3.16 ± -0.51	3.0	< 0.16	···
J1823−3021A	2.4	< 1.67	···	0.0	< 0.13	···	3.1	< 0.08	···
J1826−1256	28.6	117.49 ± 20.04	2.01 ± -0.19	7.5	< 0.46	···	0.0	< 0.14	···
J1836+5925	3177.4	409.32 ± 18.34	1.62 ± -0.06	2485.8	43.81 ± 6.54	2.80 ± -0.11	0.0	< 0.26	···
J1846+0919	0.0	< 0.67	···	0.0	< 0.13	···	0.0	< 0.07	···
J1907+0602	0.4	< 3.35	···	0.7	< 0.20	···	0.0	< 0.13	···
J1939+2134	0.0	< 1.35	···	0.0	< 0.13	···	0.0	< 0.09	···

Figure 2 shows the cutoff test...

Figure 3 shows the variability test for each source candidate. The distribution of TS_{var} is plotted in

Table 4—Continued

PSR	$TS_{0.1-1}$	$F_{0.1-1}$ (10^{-9} ph cm^{-2} s^{-1})	$\Gamma_{0.1-1}$	TS_{1-10}	F_{1-10} (10^{-9} ph cm^{-2} s^{-1})	Γ_{1-10}	TS_{10-316}	F_{10-316} (10^{-9} ph cm^{-2} s^{-1})	Γ_{10-316}
J1952+3252	6.5	< 3.50	···	6.3	< 0.14	···	0.0	< 0.09	···
J1954+2836	3.5	< 2.24	···	6.5	< 0.43	···	1.0	< 0.10	···
J1957+5033	4.3	< 0.68	···	0.0	< 0.06	···	0.0	< 0.05	···
J1958+2846	0.0	< 1.46	···	1.5	< 0.21	···	0.0	< -1000000000.00	···
J1959+2048	3.0	< 2.95	···	0.5	< 0.15	···	0.0	< 0.16	···
J2017+0603	1.9	< 0.89	···	0.0	< 0.09	···	0.0	< 0.08	···
J2021+3651	4.5	< 4.50	···	2.9	< 0.14	···	0.0	< 0.12	···
J2021+4026	1661.8	862.81 ± 42.42	1.82 ± -0.05	1175.7	69.61 ± 1.55	2.90 ± -0.02	11.5	< 0.47	···
J2028+3332	0.0	< 1.06	···	0.0	< 0.11	···	0.0	< 0.07	···
J2030+3641	0.0	< 1.16	···	0.0	< 0.09	···	0.0	< 0.05	···
J2030+4415	0.7	< 5.80	···	1.2	< 0.62	···	1.3	< 0.30	···
J2032+4127	71.2	185.44 ± 50.46	1.61 ± -0.39	55.1	26.59 ± 7.04	2.27 ± -0.25	1.1	< 0.24	···
J2043+2740	0.0	< 0.46	···	2.3	< 0.15	···	0.0	< 0.07	···
J2051−0827	0.0	< 0.52	···	0.0	< 0.06	···	0.0	< 0.07	···
J2055+2539	104.3	26.45 ± 5.37	1.61 ± -0.12	0.0	< 0.07	···	0.0	< 0.06	···
J2124−3358	18.2	< 1.87	···	120.0	2.22 ± 0.92	2.89 ± -0.30	0.0	< 0.06	···
J2139+4716	9.1	< 1.46	···	19.4	< 0.07	···	0.0	< 0.04	···
J2214+3000	1.9	< 2.48	···	0.0	< 0.24	···	0.0	< 0.28	···
J2238+5903	0.2	< 1.75	···	2.4	< 0.12	···	0.0	< 0.06	···
J2240+5832	30.9	13.32 ± 0.58	-1.09 ± -0.00	1.8	< 0.12	···	0.0	< 0.03	···
J2302+4442	61.8	25.44 ± 6.37	2.06 ± -0.27	72.5	1.69 ± 0.82	2.95 ± -0.34	0.0	< 0.05	···

Note. —

Put table comments

Table 5. Spectral fitting of pulsar wind nebula candidates with low energy component

PSR	TS_{point}	TS_{cutoff}	$F_{0.1-316}$ (10^{-9} erg cm^{-2} s^{-1})	$G_{0.1-316}$ (10^{-12} erg cm^{-2} s^{-1})	Γ	E_{cutoff} (GeV)
J0007+7303	84.0	0.0	···	···	···	···
J0034−0534	42.4	5.5	···	···	···	···
J0218+4232	34.7	2.8	···	···	···	···
J0340+4130	25.1	17.2	2.38 ± 1.52	4.95 ± 1.47	-1.20 ± 3.36	0.58 ± 0.66
J0534+2200	4959.1	0.0	···	···	···	···
J0633+1746	2842.4	176.1	711.67 ± 31.00	415.72 ± 12.92	1.40 ± 0.10	1.00 ± 0.12
J0835−4510	304.7	23.7	260.77 ± 22.71	115.15 ± 7.65	1.84 ± 0.17	1.00 ± 0.30
J1023−5746	83.0	0.0	···	···	···	···
J1119−6127	123.2	0.0	···	···	···	···
J1513−5908	122.6	0.0	···	···	···	···
J1620−4927	39.1	43.8	80.75 ± 20.97	70.24 ± 10.35	0.48 ± 0.39	0.65 ± 0.16
J1709−4429	30.7	7.4	···	···	···	···
J1744−1134	74.4	13.7	···	···	···	···
J1746−3239	47.6	33.3	64.84 ± 16.74	39.00 ± 6.10	0.79 ± 0.61	0.50 ± 0.24
J1747−2958	30.3	12.6	···	···	···	···
J1809−2332	29.0	10.8	···	···	···	···
J1813−1246	53.3	3.4	···	···	···	···
J1836+5925	5019.4	203.4	449.37 ± 14.27	330.04 ± 8.76	1.40 ± 0.03	1.64 ± 0.06
J2021+4026	920.6	138.0	949.97 ± 56.79	586.25 ± 21.87	1.64 ± 0.08	1.81 ± 0.26
J2032+4127	28.5	0.0	···	···	···	···
J2055+2539	109.0	26.3	32.23 ± 2.43	17.45 ± 1.03	1.51 ± 0.04	1.00 ± 0.04
J2124−3358	106.5	28.7	6.61 ± 2.50	9.86 ± 1.60	0.06 ± 0.92	0.87 ± 0.43
J2302+4442	115.0	12.7	···	···	···	···

Note. —

Put table comments

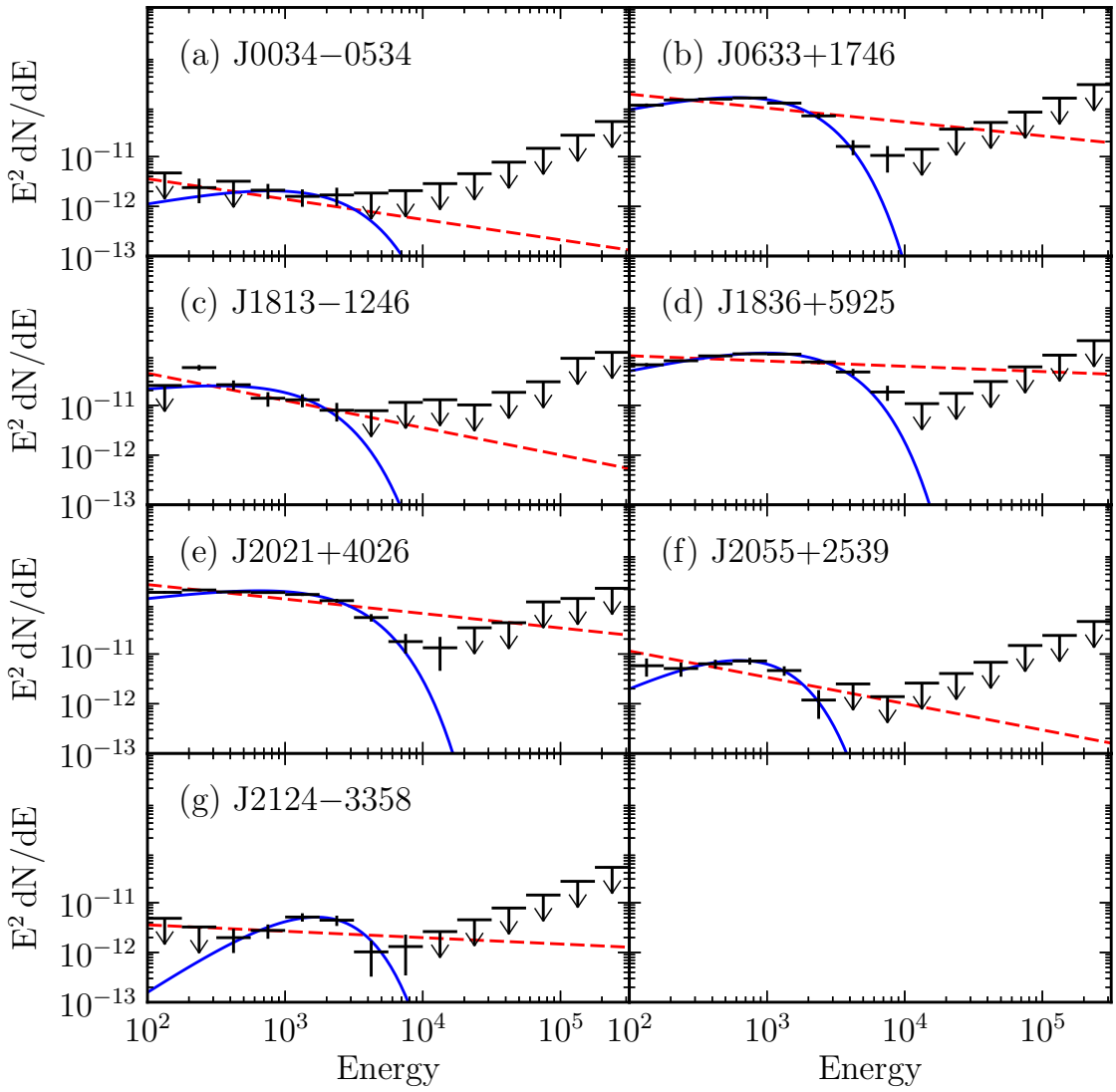

Fig. 2.— Cutoff test for some pulsars...

Table 6. Variability test

PSR	TS_{var}
J0007+7303	29.6
J0030+0451	26.6
J0034−0534	26.0
J0106+4855	0.0
J0218+4232	77.0
J0248+6021	75.4
J0340+4130	40.2
J0357+3205	0.0
J0437−4715	0.0
J0534+2200	493.7
J0610−2100	0.0
J0613−0200	19.6
J0614−3329	25.6
J0622+3749	7.1
J0631+1036	30.2
J0633+0632	7.8
J0633+1746	47.4
J0659+1414	0.0
J0729−1448	0.0
J0734−1559	29.8
J0742−2822	27.5
J0751+1807	29.6
J0835−4510	42.7
J0908−4913	33.1
J0940−5428	0.0
J1016−5857	0.0
J1019−5749	23.6
J1023−5746	45.5
J1024−0719	0.0
J1028−5819	23.6
J1044−5737	0.0
J1048−5832	0.0
J1057−5226	26.9
J1105−6107	42.9
J1119−6127	36.9
J1135−6055	7.2
J1231−1411	0.0
J1357−6429	0.0
J1410−6132	30.3
J1413−6205	0.0
J1418−6058	0.0
J1420−6048	30.5
J1429−5911	0.0
J1459−6053	0.0
J1509−5850	0.0
J1513−5908	37.5

7. Discussion

The discussion goes here...

The *Fermi* LAT Collaboration acknowledges generous ongoing support from a number of agencies and institutes that have supported both the development and the operation of the LAT as well as scientific data analysis. These include the National Aeronautics and Space Administration and the Department of Energy in the United States, the Commissariat à l'Energie Atomique and the Centre National de la Recherche Scientifique / Institut National de Physique Nucléaire et de Physique des Particules in France, the Agenzia Spaziale Italiana and the Istituto Nazionale di Fisica Nucleare in Italy, the Ministry of Education, Culture, Sports, Science and Technology (MEXT), High Energy Accelerator Research Organization (KEK) and Japan Aerospace Exploration Agency (JAXA) in Japan, and the K. A. Wallenberg Foundation, the Swedish Research Council and the Swedish National Space Board in Sweden.

Additional support for science analysis during the operations phase is gratefully acknowledged from the Istituto Nazionale di Astrofisica in Italy and the Centre National d'Études Spatiales in France.

The authors acknowledge the use of HEALPix[1] (Górski et al. 2005).

REFERENCES

Abdo, A. A., et al. 2010, ApJS, 188, 405

Górski, K. M., Hivon, E., Banday, A. J., Wandelt, B. D., Hansen, F. K., Reinecke, M., & Bartelmann, M. 2005, ApJ, 622, 759

Helene, O. 1983, Nuclear Instruments and Methods in Physics Research, 212, 319

Lande, J., et al. 2012, ApJ, in preparation

[1] `http://healpix.jpl.nasa.gov/`

Table 6—Continued

PSR	TS_{var}
J1531−5610	11.0
J1600−3053	0.0
J1614−2230	28.1
J1620−4927	45.5
J1702−4128	0.0
J1709−4429	0.0
J1713+0747	0.0
J1718−3825	14.8
J1732−3131	4.5
J1741−2054	0.0
J1744−1134	37.4
J1746−3239	37.0
J1747−2958	36.1
J1803−2149	17.1
J1809−2332	37.5
J1813−1246	39.0
J1823−3021A	14.5
J1826−1256	38.9
J1836+5925	30.6
J1846+0919	0.0
J1907+0602	0.0
J1939+2134	5.9
J1952+3252	20.1
J1954+2836	22.6
J1957+5033	0.0
J1958+2846	0.0
J1959+2048	5.8
J2017+0603	0.0
J2021+3651	55.7
J2021+4026	24.0
J2028+3332	0.0
J2030+3641	0.0
J2030+4415	26.1
J2032+4127	25.7
J2043+2740	0.0
J2051−0827	0.0
J2055+2539	67.0
J2124−3358	36.5
J2139+4716	40.8
J2214+3000	0.0
J2238+5903	0.0
J2240+5832	0.0
J2302+4442	27.9

Note. —

Put table comments

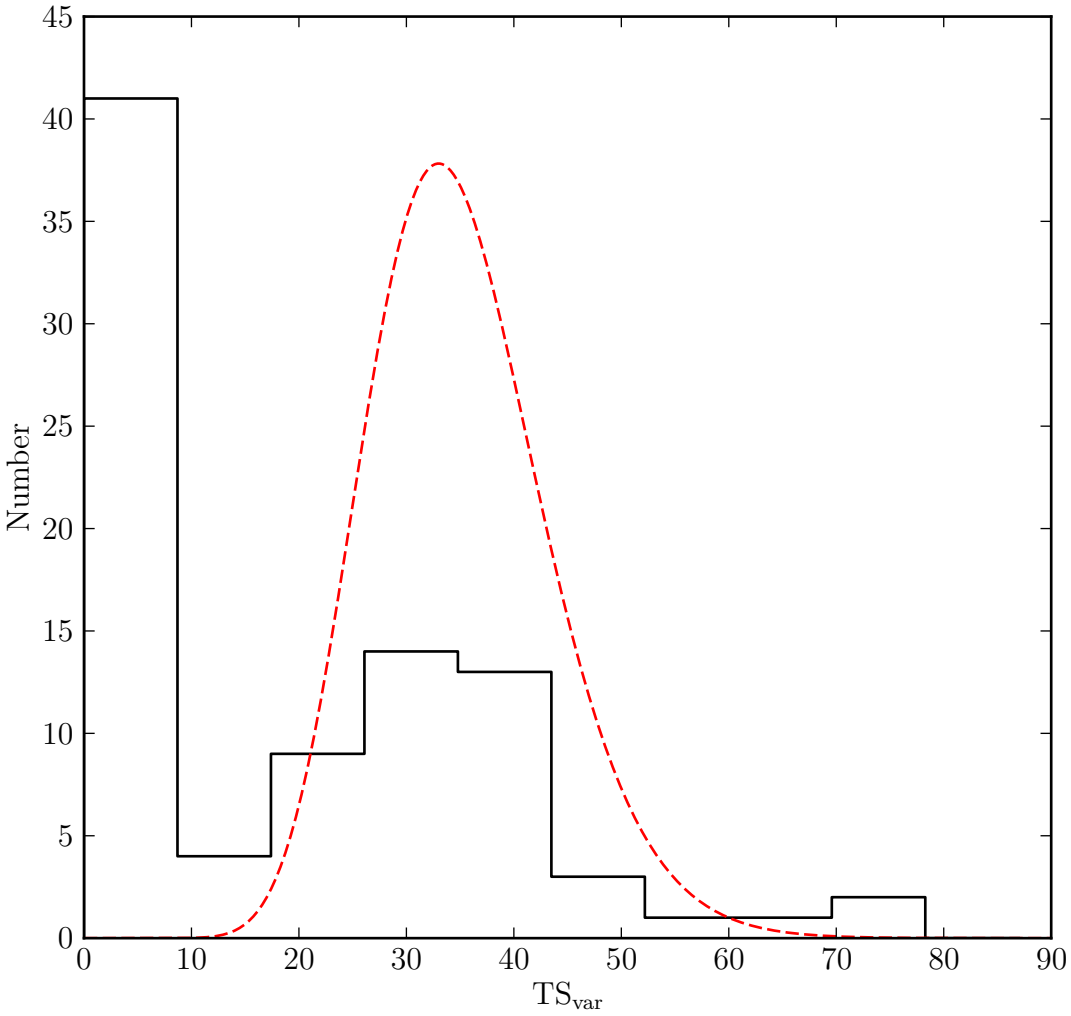

Fig. 3.— Distribution of TS_{var} for each source candidate.

Disclaimer about crab not being included

.

A. Validation of Extension Upper Limits

For sources that are significantly detected but that do not have a significantly-detectable extension, it can often interesting to derive an upper limit on any possible extension for the source. Here, we present an algorithm for obtaining an upper limit on the extension of a currently unresolved source using a a Bayesian method proposed by Helene (Helene 1983). The same algorithm has been used by the *Fermi*-LAT collaboration to obtain upper limits on the flux of point-like sources not significantly detected at GeV energies. See for example Abdo et al. (2010).

In this method, we assume a particular spatial shape for the currently-unresolved source (for example a uniform disk spatial distribution) and we profile over the extension of the currently-unresolved source. For simplicty, we assume this spatial shape is defined by a single extension parameter σ.

For a given extension, the spectral parameters of the source as well as other nearby sources and diffuse backgrounds are maximized to obtain the likelihood as a function of extension $\mathcal{L}(\sigma)$. The 95% confidence upper limits σ_{ul} on the extension of a source is obtained by finding the extension σ such that

$$\int_0^{\sigma_{ul}} \mathcal{L}(\sigma) = 0.95 \tag{A1}$$

assuming that the likelihood is normalized such that

$$\int_0^{\infty} \mathcal{L}(\sigma) = 1 \tag{A2}$$

For compulational efficienciy, this upper limit algorithm was implemented in `pointlike` which introduces negligible approximations what make this alogirhtm compultationally tractable (Lande et al. 2012). Something about how this is biased by not marginalizing over the position of the extended source, but that this is not a huge effect

To validate this method, we performed a monte carlo study of the coverage of the extension upper limits. Because the method is Bayesian, it has to overcover for arbitrarily small extensions. On the other hand, it is reasonable to expect the method to correctly cover for larger sources.

For simplicity, In our simulation we used the same time range and background model described in section 4 of **?**. In particular, our simulations were performed assuming the 2FGL pointing history against an isotropic background consistent with the isotropic background measured by EGRET.

We were interseted in verying the extension upper limits in two distincy energy ranges, first for sources just on the edge of detectability (as pointlike) which could potentially be extended. We picked for spectral indices varying from 1.5 to 4 and extensions varying from $0\overset{\circ}{.}0$ to $2\overset{\circ}{.}0$. We selected fluxes so that $\mathrm{TS}_{\mathrm{point}} \sim 35$ for a given flux and extension. Figure 4 shows this monte carlo study.

The second simulation concerns sources that are very significant, comparable in brightness to, for example, the Crab Nebula but that cannot be spatially resolved. Figure 5 shows this monte carlo study.

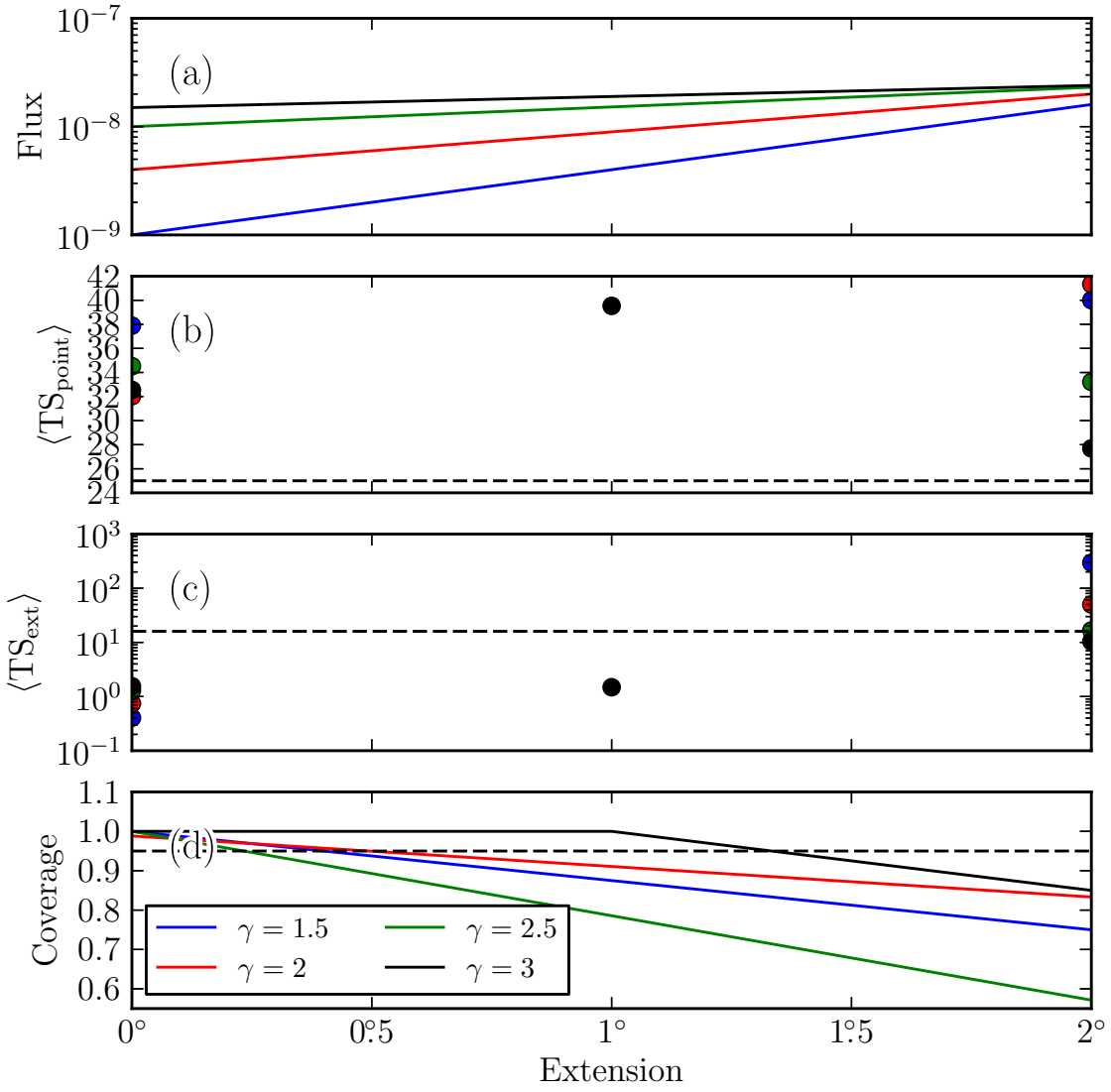

Fig. 4.— Monte carlo study.

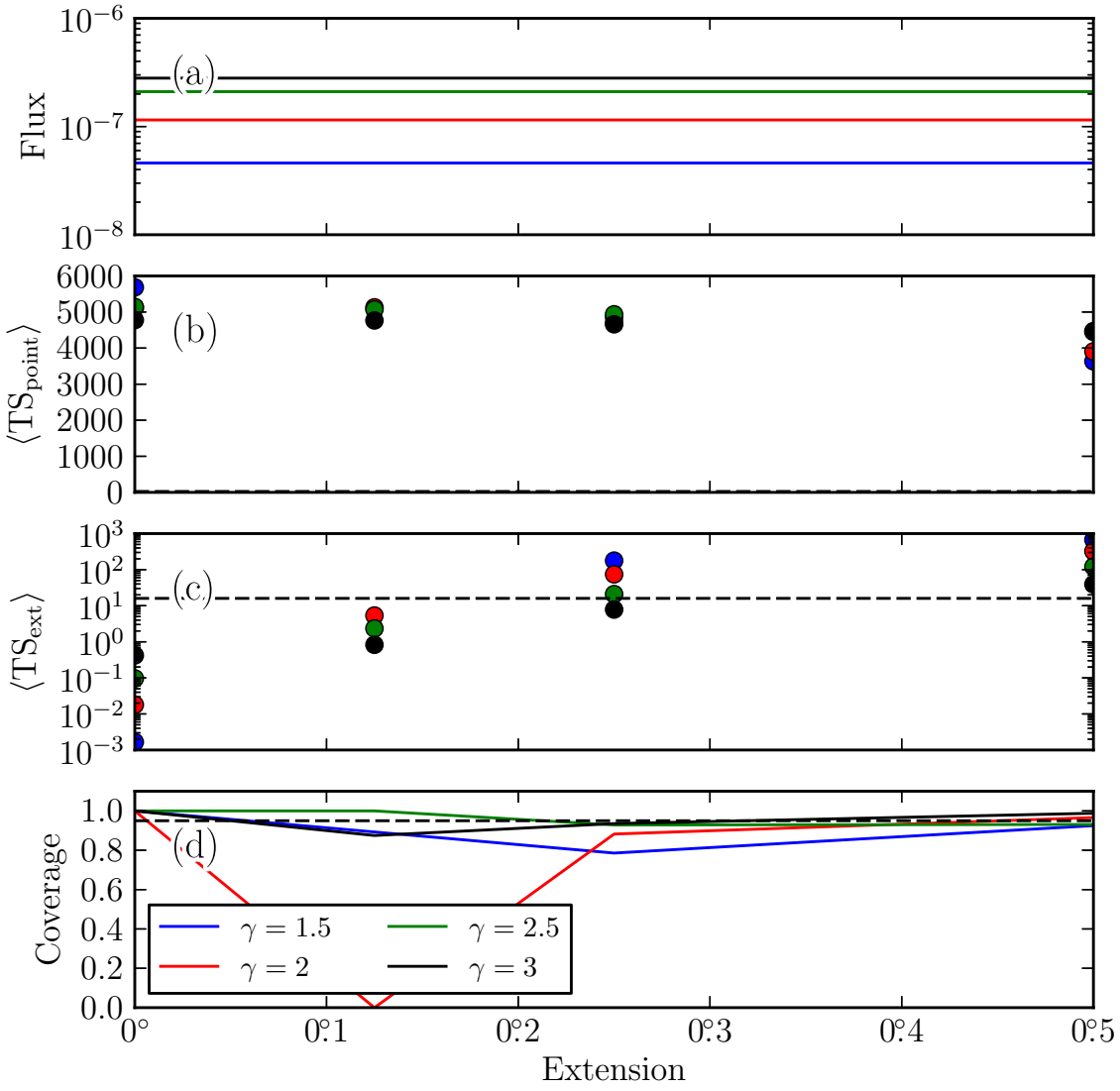

Fig. 5.— Extension upper limit stuff.